THE JOURNAL OF BIOLOGICAL CHEMISTRY
Vol. 273, No. 33, Issue of August 14, pp. 21161–21168, 1998

Printed in U.S.A.

Overexpression of a DEAD Box Protein (DDX1) in Neuroblastoma and Retinoblastoma Cell Lines*

(Received for publication, November 17, 1997, and in revised form, June 2, 1998)

Roseline Godbout‡, Mary Packer, and Wenjun Bie

From the Department of Oncology, Cross Cancer Institute and University of Alberta, 11560 University Ave., Edmonton, Alberta T6G1Z2, Canada

The DEAD box gene, *DDX1*, is a putative RNA helicase that is co-amplified with *MYCN* in a subset of retinoblastoma (RB) and neuroblastoma (NB) tumors and cell lines. Although gene amplification usually involves hundreds to thousands of kilobase pairs of DNA, a number of studies suggest that co-amplified genes are only overexpressed if they provide a selective advantage to the cells in which they are amplified. Here, we further characterize *DDX1* by identifying its putative transcription and translation initiation sites. We analyze DDX1 protein levels in *MYCN*/*DDX1*-amplified NB and RB cell lines using polyclonal antibodies specific to DDX1 and show that there is a good correlation with *DDX1* gene copy number, *DDX1* transcript levels, and DDX1 protein levels in all cell lines studied. DDX1 protein is found in both the nucleus and cytoplasm of *DDX1*-amplified lines but is localized primarily to the nucleus of nonamplified cells. Our results indicate that DDX1 may be involved in either the formation or progression of a subset of NB and RB tumors and suggest that DDX1 normally plays a role in the metabolism of RNAs located in the nucleus of the cell.

DEAD box proteins are a family of putative RNA helicases that are characterized by eight conserved amino acid motifs, one of which is the ATP hydrolysis motif containing the core amino acid sequence DEAD (Asp-Glu-Ala-Asp) (1–3). Over 40 members of the DEAD box family have been isolated from a variety of organisms including bacteria, yeast, insects, amphibians, mammals, and plants. The prototypic DEAD box protein is the translation initiation factor, eukaryotic initiation factor 4A, which, when combined with eukaryotic initiation factor 4B, unwinds double-stranded RNA (4). Other DEAD box proteins, such as p68, Vasa, and An3, can effectively and independently destabilize/unwind short RNA duplexes *in vitro* (5–7). Although some DEAD box proteins play general roles in cellular processes such as translation initiation (eukaryotic initiation factor 4A (4)), RNA splicing (PRP5, PRP28, and SPP81 in yeast (8–10)), and ribosomal assembly (SrmB in *Escherichia coli* (11)), the function of most DEAD box proteins remains unknown. Many of the DEAD box proteins found in higher eukaryotes are tissue- or stage-specific. For example, *PL10* mRNA is expressed only in the male germ line, and its product has been proposed to have a specific role in translational regulation during spermatogenesis (12). Vasa and ME31B are maternal proteins that may be involved in embryogenesis (13, 14). p68, found in dividing cells (15), is believed to be required for the formation of nucleoli and may also have a function in the regulation of cell growth and division (16, 17). Other DEAD box proteins are implicated in RNA degradation, mRNA stability, and RNA editing (18–20).

The human DEAD box protein gene *DDX1*[1] was identified by differential screening of a cDNA library enriched in transcripts present in the two RB cell lines Y79 and RB522A (21). The longest *DDX1* cDNA insert isolated from this library was 2.4 kb with an open reading frame from position 1 to 2201. All eight conserved motifs characteristic of DEAD box proteins are found in the predicted amino acid sequence of DDX1 as well as a region with homology to the heterogeneous nuclear ribonucleoprotein U, a protein believed to participate in the processing of heterogeneous nuclear RNA to mRNA (22, 23). The region of homology to heterogeneous nuclear ribonucleoprotein U spans 128 amino acids and is located between the first two conserved DEAD box protein motifs, 1a and 1b.

The proto-oncogene *MYCN* encodes a member of the MYC family of transcription factors that bind to an E box element (CACGTG) when dimerized with the MAX protein (24, 25). The *MYCN* gene is amplified and overexpressed in approximately one-third of all NB tumors (26, 27). Amplification of *MYCN* is associated with rapid tumor progression and a poor clinical prognosis (26, 27). MYCN overexpression is usually achieved by increasing gene copy number rather than by up-regulating basal expression of MYCN (27, 28). Because gene amplification involves hundreds to thousands of kilobase pairs of contiguous DNA (29–32), it is possible that co-amplification of a gene located in proximity to *MYCN* may contribute to the poor clinical prognosis of *MYCN*-amplified tumors. The *DDX1* gene maps to the same chromosomal band as *MYCN*, 2p24, and is located ~400 kb telomeric to the *MYCN* gene (33–36). All four *MYCN*-amplified RB tumor cell lines tested to date are amplified for *DDX1* (21),[2] while approximately two-thirds of NB cell lines and 38–68% of NB tumors are co-amplified for both genes (37–39). George *et al*. (39) found a significant decrease in the mean disease-free survival of patients with *DDX1*/*MYCN*-amplified NB tumors compared with *MYCN*-amplified tumors. Similarly, Squire *et al*. (38) observed a trend toward a worse clinical prognosis when both genes were amplified in the tumors of NB patients. To date, there have been no reports of a

* This work was supported by the National Cancer Institute of Canada with funds from the Canadian Cancer Society. The costs of publication of this article were defrayed in part by the payment of page charges. This article must therefore be hereby marked "*advertisement*" in accordance with 18 U.S.C. Section 1734 solely to indicate this fact.

The nucleotide sequence(s) reported in this paper has been submitted to the GenBank™/EBI Data Bank with accession number(s) X70649.

‡ To whom correspondence should be addressed: Dept. of Oncology, Cross Cancer Institute, 11560 University Ave., Edmonton, Alberta T6G 1Z2, Canada. Tel.: 403-432-8901; Fax: 403-432-8892.

[1] The abbreviations used are: DDX1, DEAD box 1; NB, neuroblastoma; RB, retinoblastoma; RACE, rapid amplification of cDNA ends; PAGE, polyacrylamide gel electrophoresis; nt, nucleotide(s); MOPS, 4-morpholinepropanesulfonic acid; bp, base pair(s); kb, kilobase(s) or kilobase pair(s).

[2] R. Godbout, unpublished results.

tumor amplified only for *DDX1*, and the role that this gene plays in cancer formation and progression is not known.

Because of the high rate of rearrangements in amplified DNA (31, 40), it is unlikely that a gene located ~400 kb from the *MYCN* gene will be consistently amplified as an intact unit unless its product provides a growth advantage to the cell. Based on Southern blot analysis, the *DDX1* gene extends over more than 30 kb, and there are no gross rearrangements of this gene in *DDX1*-amplified tumors (21, 38). Furthermore, there is a good correlation between *DDX1* transcript levels and gene copy number in the tumors analyzed to date. However, we need to show that DDX1 protein is overexpressed in *DDX1*-amplified tumors if we are to entertain the possibility that this protein plays a role in the tumorigenic process. Here, we isolate and characterize the 5′-end of *DDX1* mRNA and extend the *DDX1* cDNA sequence by ~300 nt. We identify the predicted initiation codon of DDX1 and generate antisera that specifically recognize DDX1 protein. We analyze levels of DDX1 protein in both *DDX1*-amplified and nonamplified RB and NB tumors and study the subcellular location of this protein in the cell.

MATERIALS AND METHODS

Library Screening—A human fetal brain cDNA library (Stratagene) was screened using a 320-bp DNA fragment from the 5′-end of the 2.4-kb *DDX1* cDNA previously described (23). Phagemids containing positive inserts were excised from λ ZAP II following the supplier's directions. The ends of the cDNA inserts were sequenced using the dideoxynucleotide chain termination method with T7 DNA polymerase (Amersham Pharmacia Biotech).

A human placenta genomic library (CLONTECH) was screened with the 5′-end of *DDX1* cDNA. Positive plaques were purified, and the genomic DNA was analyzed using restriction enzymes and Southern blotting. *Eco*RI-digested DNA fragments from these clones were subcloned into pBluescript and digested with exonuclease III and mung bean nuclease to obtain sequentially deleted clones. The exon/intron map of the 5′ portion of the *DDX1* gene was obtained by comparing the sequence of *DDX1* cDNA with that of the genomic DNA.

Rapid Amplification of cDNA Ends (RACE)—We used the AmpliFINDER RACE kit (CLONTECH) to extend the 5′-end of *DDX1* cDNA. Briefly, two μg of poly(A)$^+$ RNA isolated from RB522A was reverse transcribed at 52 °C using either primer P1 or P3 (Fig. 1*A*). The RNA template was hydrolyzed, and excess primer was removed. A single-stranded AmpliFINDER anchor containing an *Eco*RI site was ligated to the 3′-end of the cDNA using T4 RNA ligase. The cDNA was amplified using either primer P2 or P4 (Fig. 1*A*) and AmpliFINDER anchor primer. RACE products were cloned into pBluescript.

Primer Extension—Poly(A)$^+$ RNAs were isolated from RB and NB cell lines as described previously (21, 38). The 21-nt primers 5′-TTCGTTCTGGGCACCATGTGT-3′ (primer P4 in Fig. 1*A*) and 5′-TGGGACCTAGGGCTTCTGGAC-3′ (primer P3 in Fig. 1*A*) were end-labeled with [γ-^{32}P]ATP (3000 Ci/mmol; Mandel Scientific) and T4 polynucleotide kinase. Each of the labeled primers was annealed to 2 μg of poly(A)$^+$ RNA at 45 °C for 90 min, and the cDNA was extended at 42 °C for 60 min using avian myeloblastosis virus reverse transcriptase (Promega). The primer extension products were heat-denatured and run on a 8% polyacrylamide gel containing 7 M urea in 1× TBE buffer. A G + A sequencing ladder served as the size standard.

S1 Nuclease Protection Assay—The S1 nuclease protection assay to map the transcription initiation site of *DDX1* was performed as described by Favaloro *et al.* (41). The DNA probe was prepared by digesting genomic DNA spanning the upstream region of *DDX1* and exon 1 with *Ava*I, labeling the ends with [γ-^{32}P]ATP (3000 Ci/mmol) and polynucleotide kinase, and removing the label from one of the ends by digesting the DNA with *Sph*I (Fig. 4). The RNA samples were resuspended in a hybridization mixture containing 80% formamide, 40 mM PIPES, 400 mM NaCl, 1 mM EDTA, and the heat-denatured *Sph*I–*Ava*I probe labeled at the *Ava*I site. The samples were incubated at 45 °C for 16 h and digested with 3000 units/ml S1 nuclease (Boehringer Mannheim) for 60 min at 37 °C. The samples were precipitated with ethanol; resuspended in 80% formaldehyde, TBE buffer, 0.1% bromphenol blue, xylene cyanol; denatured at 90 °C for 2 min; and electrophoresed in a 7 M urea, 8% polyacrylamide gel in TBE buffer.

Northern and Southern Blot Analysis—Poly(A)$^+$ RNAs were isolated from RB and NB cell lines as described previously (21, 38). Two μg of poly(A)$^+$ RNA/lane were electrophoresed in a 6% formaldehyde, 1.5% agarose gel in MOPS buffer (20 mM MOPS, 5 mM sodium acetate, 1 mM EDTA, pH 7.0) and transferred to nitrocellulose filter in 3 M sodium chloride, 0.3 M sodium citrate. The filters were hybridized to the following DNA probes, ^{32}P-labeled by nick translation: (i) a 1.6-kb *Eco*RI insert from *DDX1* cDNA clone 1042 (21), (ii) a 260-bp cDNA fragment spanning the 3′-end of *DDX1* exon 1 as well as exons 2 and 3, (iii) a 160-bp fragment derived from the 5′-end of *DDX1* exon 1, and (iv) α-actin cDNA to control for lane to lane variation in RNA levels. Filters were hybridized and washed under high stringency. Southern blot analysis was as described previously (21).

Preparation of Anti-DDX1 Antiserum—To prepare antiserum to the C terminus of the DDX1 protein, we inserted a 1.8-kb *Eco*RI fragment from bp 848 to 2668 of *DDX1* cDNA (Fig. 1*B*) into *Eco*RI-digested pMAL-c2 expression vector (New England Biolabs). DH5α cells transformed with this vector were grown to mid-log phase and induced with 0.1 mM isopropyl-1-thio-β-D-thiogalactoside. The cells were harvested 3–4 h postinduction and lysed by sonication. Soluble maltose binding protein-DDX1 fusion protein was affinity-purified using amylose resin, and the maltose-binding protein was cleaved with factor Xa. The DDX1 protein was purified on a SDS-PAGE gel, electroeluted, and concentrated. Approximately 100 μg of protein was injected into rabbits at 4–6-week intervals. For the initial injection, the protein was dispersed in complete Freund's adjuvant (Sigma), while subsequent injections were prepared in Freund's incomplete adjuvant. Blood was collected from each rabbit 10 days after injection, and the specificity of the antiserum was tested using cell extracts from RB522A. To prepare antiserum to the N terminus of DDX1 protein, a *DDX1* cDNA fragment from bp 268 to 851 (Fig. 1*B*) was inserted into pGEX-4T2 (Amersham Pharmacia Biotech). The recombinant protein produced from this construct contains the first 186 amino acids of the predicted DDX1 sequence. Soluble glutathione *S*-transferase-DDX1 fusion protein was purified with glutathione-Sepharose 4B (Amersham Pharmacia Biotech). The glutathione *S*-transferase component of the fusion protein was cleaved with thrombin.

Subcellular Fractionations and Western Blot Analysis—We used two different procedures for subcellular fractionations. First, we isolated nuclear and S100 (soluble cytoplasmic) fractions from RB522A, IMR-32, Y79, RB(E)-2, HeLa, and HL60 using the procedure of Dignam (42). On average, we obtained 5–6 times more protein in the cytosolic fractions than in the nuclear fractions. Second, 10^8 RB522A cells were lysed and fractionated into S4 (soluble cytoplasmic components), P2 (heavy mitochondria, plasma membrane fragments), P3 (mitochondria, lysozymes, peroxisomes, and Golgi membranes), and P4 fractions (membrane vesicles from rough and smooth endoplasmic reticulum, Golgi, and plasma membrane) by differential centrifugation (43). We obtained 8 mg of protein in the S4 fraction, 1 mg in P2, 0.5 mg in P3, and 2 mg in P4 fraction. The procedures related to the immunoelectron microscopy have been previously described (44).

For Western blot analysis, proteins were electrophoresed in polyacrylamide-SDS gels and electroblotted onto nitrocellulose using the standard protocol for protein transfer described by Schleicher and Schuell. The filters were incubated with a 1:5000 dilution of DDX1 antiserum, a 1:200 dilution of anti-MYCN monoclonal antibody (Boehringer Mannheim), or a 1:200 dilution of anti-actin (Santa Cruz Biotechnology, Inc., Santa Cruz, CA). For the colorimetric analysis, antigen-antibody interactions were visualized using either alkaline phosphatase-linked goat anti-rabbit IgG (for DDX1) or goat anti-mouse IgG (for MYCN) at a 1:3000 dilution. For the ECL Western blotting analysis (Amersham Pharmacia Biotech), we used a 1:100,000 dilution of peroxidase-linked secondary anti-rabbit IgG antibody (for DDX1) or secondary anti-goat IgG antibody (Jackson ImmunoResearch Laboratories).

RESULTS

Identification of the 5′-End of the DDX1 Transcript—We have previously reported the sequence of *DDX1* cDNA isolated from an RB cDNA library (21, 23). This 2.4-kb *DDX1* cDNA contains an open reading frame spanning positions 1–2201 with a methionine encoded by the first three nucleotides (Fig. 1*A*). There is a polyadenylation signal and poly(A) tail in the 3′-untranslated region, indicating that the sequence is complete at the 3′-end. Manohar *et al.* (37) have also isolated *DDX1* cDNA from the NB cell line LA-N-5. Their cDNA extended the 5′-end of our sequence by 42 bp and included an additional in frame methionine (*double underlined* in Fig. 1*A*). The possibil-

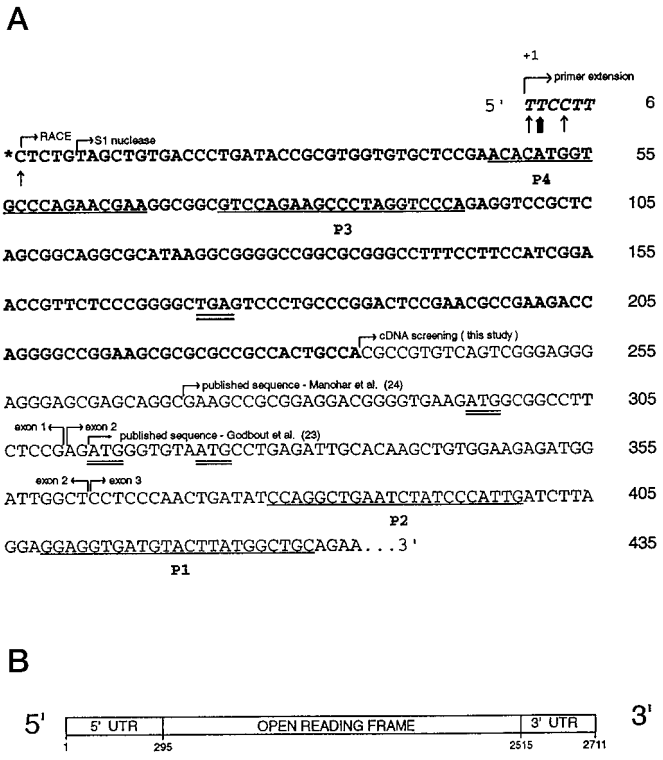

FIG. 1. **Partial sequence and structure of *DDX1* cDNA.** *A*, the sequence of the 5′-end of *DDX1* cDNA. The sequence in *boldface type* starting at the *asterisk* was obtained using the RACE strategy. The additional 6 bp in *italic boldface type* at the 5′-end of the cDNA are predicted based on the known *DDX1* genomic sequence and primer extension analysis. P1, P2, P3, and P4 are primers used in the RACE experiments (the complementary sequence was used in each case). Primers P3 and P4 were also used for the primer extension analysis. Three in frame methionine codons are indicated by the *double underline*. An in frame stop codon is indicated by the *boldface double underline*. The three major transcription initiation sites identified by primer extension are indicated by the *single arrows*, while a minor site is represented by the *broad arrow*. The predicted *DDX1* transcription initiation sites obtained by RACE, S1 nuclease, and primer extension are indicated as well as the 5′-ends of *DDX1* cDNA sequences obtained by screening cDNA libraries. The sequences transcribed from exons 1, 2, and 3 are also shown. *B*, the structure of the 2711-bp *DDX1* cDNA is shown with an open reading frame from position 295 to 2515.

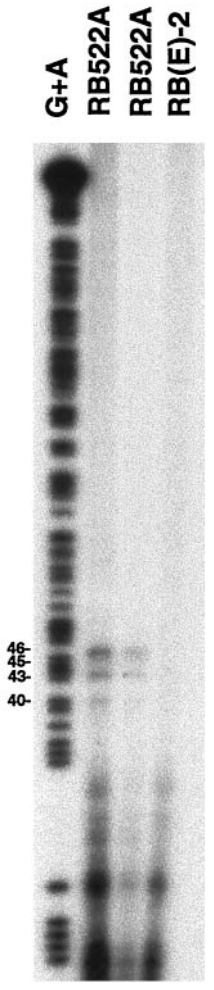

FIG. 2. **Identification of the 5′-end of the *DDX1* transcript by primer extension.** Radioactively labeled primer P4 was annealed to 2 μg of poly(A)$^+$ RNA from RB522A (*lane 1*), 1 μg of poly(A)$^+$ RNA from RB522A (*lane 2*), and 2 μg of poly(A)$^+$ RNA from RB(E)-2 cells (*lane 3*), and extended using reverse transcriptase. The products were run on an 8% denaturing polyacrylamide gel with a G + A sequencing ladder as size marker. The primer extension products are indicated on the *left*. The sizes of the products (in nt) are presented as the distance from primer P4.

ity of additional in frame methionines located further upstream could not be excluded, because there were no predicted stop codons in the upstream region of the cDNA.

Northern blot analysis indicated a *DDX1* transcript size of ~2800 nt, suggesting that the *DDX1* cDNAs isolated to date were lacking ~300–350 bp of 5′ sequence. We have used different approaches to identify the transcription start site of *DDX1*. First, we exhaustively screened a commercial fetal brain cDNA library with the 5′-end of *DDX1* cDNA. Although numerous clones were analyzed, only one extended the sequence (by 35 bp) beyond that published by Manohar *et al.* (37) (Fig. 1*A*).

We next used the RACE procedure in an attempt to isolate additional 5′ sequence. The nested primers used to amplify the 5′-end of the *DDX1* transcript are labeled as primers P1 and P2 in Fig. 1*A* and are located downstream of the three in frame methionines (*double underlined* in Fig. 1*A*). Poly(A)$^+$ RNA from RB522A was reverse transcribed at 52 °C using primer P1, and the reverse transcribed cDNA was amplified using the nested primer P2 and the 5′-RACE primer. Using this approach, we generated a product that was 230 bp longer than any of the cDNAs obtained by screening libraries (Fig. 1*A*). Sequencing of this 230-bp cDNA revealed an in frame stop codon (*boldface double underline* in Fig. 1*A*) located 123 bp upstream of the predicted translation initiation site. We then prepared primers P3 and P4, located near the 5′-end of the RACE cDNA (Fig. 1*A*) and repeated the RACE procedure to see if additional 5′ sequences could be obtained. The resulting RACE products did not extend the *DDX1* cDNA sequence further.

The location of the *DDX1* transcription initiation site was verified by primer extension. Poly(A)$^+$ RNA was prepared from the following two cell lines: *DDX1*-amplified RB cell line RB522A and a nonamplified RB cell line RB(E)-2. RB522A has elevated levels of *DDX1* mRNA, while RB(E)-2 has at least 20-fold lower levels of this transcript. Three products of 40, 43, and 46 nt (with a weak signal at 45 nt) were detected in RB522A using primer P4 (Figs. 1*A* and 2). The 40-nt product corresponded exactly with the 5′-end of the RACE-derived cDNA while the 43- and 46-nt products extended the predicted size of the *DDX1* transcript by 3 and 6 nt, respectively. None of these products were observed in RB(E)-2. Bands of identical sizes to those obtained with RB522A mRNA were also observed in the *DDX1*-amplified NB cell line BE(2)-C but not in the *DDX1*-amplified NB cell line IMR-32 (data not shown). The same predicted *DDX1* transcription initiation site was identified with primer P3 except that the bands were of weaker

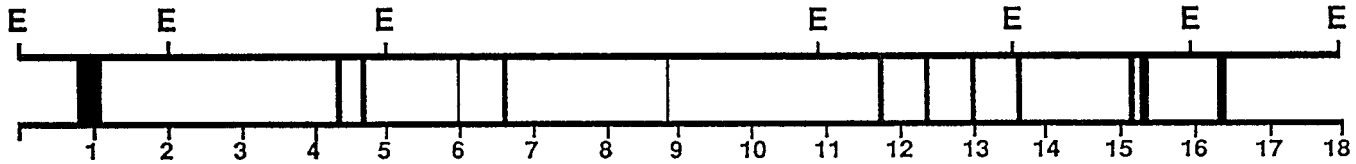

FIG. 3. **Genomic map of the 5′-end of *DDX1*.** The exons are represented by the *black boxes*, and distances are in kilobase pairs. The locations of *Eco*RI (*E*) sites are indicated.

intensity (data not shown). We have designated the transcription start site identified by primer extension as +1 (Fig. 1*A*).

The sequence of the 6 nt extending beyond the RACE cDNA was obtained by comparison of the cDNA sequence with that of *DDX1* genomic DNA. Bacteriophages containing *DDX1* genomic DNA were isolated by screening a human placenta library with 5′ *DDX1* cDNA. Eighteen kb of DNA were sequenced from two bacteriophages with overlapping *DDX1* genomic DNA. Thirteen exons were identified within this 18-kb region (Fig. 3) corresponding to cDNA sequences from position 1 to 1249. The 310-bp exon 1 was by far the longest of the 13 exons sequenced, corresponding to the entire 5′-untranslated region of *DDX1* as well as the first in frame methionine. The sequences transcribed from exons 1, 2, and 3 are indicated in Fig. 1*A*.

Knowledge of the genomic structure of *DDX1* allowed us to use the S1 protection assay, a technique that is independent of reverse transcriptase, to further define the 5′-end of the *DDX1* transcript. Poly(A)$^+$ RNAs from six *DDX1*-amplified lines (RB lines: Y79 and RB522A; NB lines: BE(2)-C, IMR-32, LA-N-1, and LA-N-5) and six nonamplified lines (RB lines: RB(E)-2 and RB412; NB lines, GOTO, NB-1, NUB-7, and SK-N-MC) were hybridized to a DNA probe that extended from position −745 in the 5′-flanking *DDX1* DNA to position +164 in exon 1. This DNA probe was labeled at position +164 as indicated in Fig. 4. Nonhybridized DNA was digested with S1 nuclease, and the sizes of the protected fragments were analyzed on a denaturing polyacrylamide gel. Bands of 150–153 nt were observed in *lane 2* (RB522A), *lane 5* (BE(2)-C), and *lane 8* (LA-N-1) with bands of much weaker intensity in *lane 7* (IMR-32) (Fig. 4). Specific bands were not detected in either *DDX1*-amplified Y79 and LA-N-5 or the nonamplified lines. Although the sizes of the S1 protected bands in RB522A, BE(2)-C, and LA-N-1 were 5 and 11 nt shorter than predicted based on RACE and primer extensions, respectively, there was general agreement with all three techniques regarding the location of the *DDX1* transcription initiation site (Fig. 1*A*). The smaller S1 nuclease protected products could have arisen as the result of S1 digestion of the 5′-end of the RNA:DNA heteroduplex because of its relatively high rU:dA content (45).

Identification of the same transcription initiation site in three *DDX1*-amplified lines suggests that this represents the bona fide start site of *DDX1* transcription. However, it was not clear why this start site was either very weak or not detected in three other amplified lines. To determine whether the 5′-end of exon 1 is transcribed in all *DDX1*-amplified lines, we carried out a direct analysis of the 5′-end of the *DDX1* transcript by Northern blotting. Two probes were used for this analysis: the 5′ probe contained a 160-bp fragment from bp 1 to 160 (5′-half of exon 1), and the 3′ probe contained a 260-bp fragment from bp 160 to 420 (3′-half of exon 1 as well exons 2 and 3) (Fig. 1*A*). With the 3′ probe, we obtained bands of similar size and intensity in four *DDX1*-amplified lines (RB522A, BE(2)-C, IMR-32, and LA-N-5). Band intensity was somewhat weaker in Y79 and stronger in LA-N-1 in comparison with the other lines (Fig. 5). No signal was detected in the non-*DDX1*-amplified line RB412. With the 5′ probe, a relatively strong signal was observed in RB522A, BE(2)-C, and LA-N-1, while a considerably weaker but readily apparent signal was detected in Y79, IMR-32, and LA-N-5. The signal obtained with actin indicates that, with the exception of LA-N-1, similar amounts of RNA were loaded in each lane and that the RNA was not degraded. These results indicate that at least a portion of the 160-bp 5′-end of exon 1 is transcribed in all *DDX1*-amplified lines.

Based on primer extension, S1 nuclease protection assay, Northern blot analysis and the sequencing of the RACE products, we conclude that the *DDX1* transcript is 2.7 kb with an open reading frame spanning nucleotides 295–2515 encoding a predicted protein of 740 amino acids with an estimated molecular weight of 82.4 (Fig. 1*B*). An in frame stop codon is located 123 nt upstream of the predicted translation initiation site, at positions 172–174. The first in frame methionine following the stop codon is in agreement with the Kozak consensus sequence (46). Furthermore, the predicted start methionine codon for human DDX1 corresponds perfectly with that of *Drosophila* DDX1 (47). A stop codon is located 15 nt upstream of the initiation codon in *Drosophila* DDX1.

Analysis of DDX1 Protein Levels in Neuroblastoma and Retinoblastoma—We and others have previously shown that there is a good correlation between gene copy number and RNA levels in *DDX1*-amplified RB and NB cell lines (37, 38). To determine whether the correlation extends to DDX1 protein levels, we prepared antiserum to two nonoverlapping recombinant DDX1 proteins. First, we prepared a C terminus recombinant protein construct by inserting a 1.8-kb *Eco*RI fragment from bp 848 to 2668 (amino acids 185–740) (Fig. 1*B*) into the pMAL-c2 expression vector. Recombinant protein expression was induced with isopropyl-1-thio-β-D-thiogalactoside, and the 110-kDa maltose-binding protein-DDX1 fusion product was purified by affinity chromatography using amylose resin, followed by electrophoresis on a SDS-PAGE gel after cleaving the maltose-binding protein fusion partner with factor Xa. Second, we prepared an N terminus construct by ligating a DNA fragment from bp 268 to 851 (amino acids 1–186) into pGEX-4T2. The 50-kDa glutathione *S*-transferase-DDX1 fusion protein was purified by affinity chromatography on a glutathione column. This N terminus fusion protein contains only the first of the eight conserved motifs found in all DEAD box proteins, while the C terminus fusion protein includes the remaining seven motifs.

We measured DDX1 protein levels in total cell extracts of three RB and 10 NB cell lines. Using antiserum to the N terminus fusion protein, we observed a strong signal in all *DDX1*-amplified cell lines: the RB cell lines Y79 (*lane 1*) and RB522A (*lane 2*) and the NB cell lines BE(2)-C (*lane 4*), IMR-32 (*lane 6*), LA-N-1 (*lane 8*), and LA-N-5 (*lane 9*) (Fig. 6). Two bands were observed in the majority of extracts. Of the amplified lines, Y79 produced the weakest signal, with the most intense signal observed in LA-N-1. There was an excellent correlation with DDX1 protein and mRNA levels in these cell lines, with lower levels of DDX1 mRNA observed in Y79 and higher levels in LA-N-1 (Fig. 7*A*). As shown in Fig. 7*B*, this correlation extended to *DDX1* gene copy number. No gross DNA rearrangements were seen in the *DDX1*-amplified lines; however, three small bands of altered size were observed in the RB412 lane. Although the nature of the DNA alteration is not known, it is noteworthy that *DDX1* transcript levels in RB412

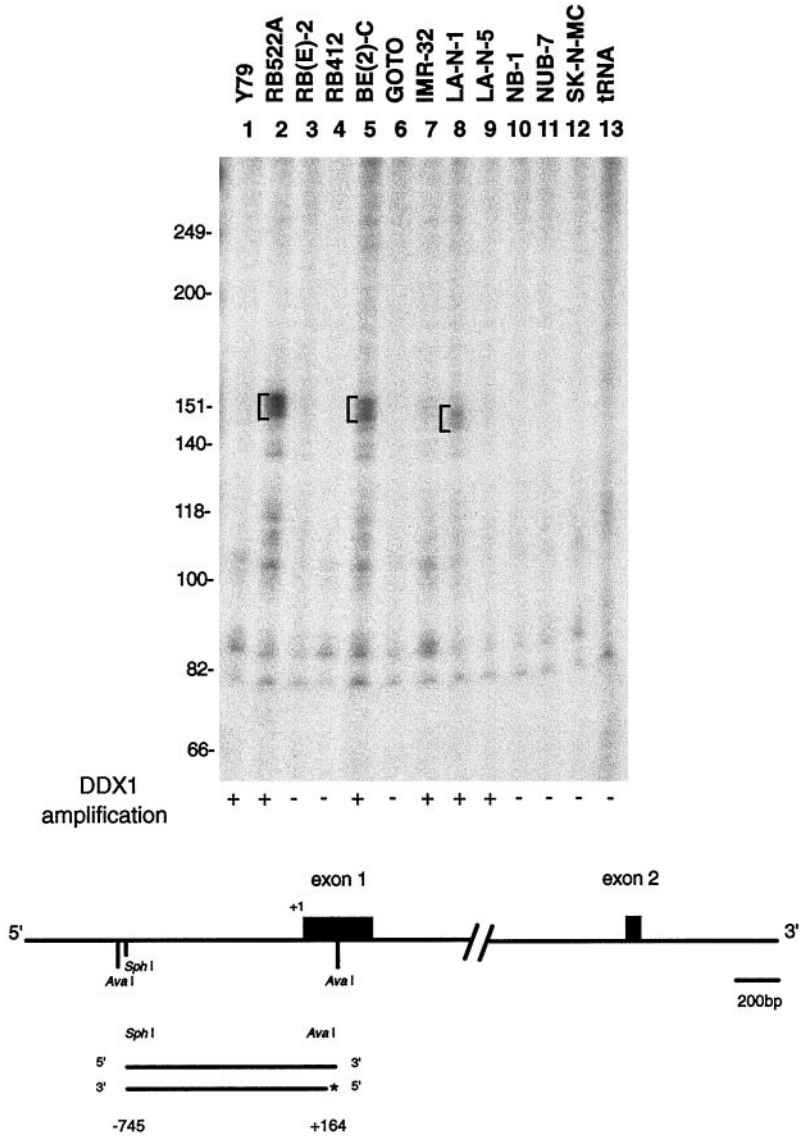

FIG. 4. **S1 nuclease mapping of the 5′-end of the *DDX1* transcript.** Two μg of poly(A)$^+$ RNA from four RB lines (*DDX1*-amplified Y79 and RB522A and nonamplified RB(E)-2 and RB412), eight NB lines (*DDX1*-amplified BE(2)-C, IMR-32, LA-N-1, and LA-N-5 and nonamplified GOTO, NB-1, NUB-7, and SK-N-MC), and tRNA as a negative control were hybridized to a *Sph*I–*Ava*I fragment labeled at the *Ava*I site with [γ-^{32}P]ATP and polynucleotide kinase. Bands of 150–153 nt are shown in *lanes 2* (RB522A), *5* (BE(2)-C), and *8* (LA-N-1) with much weaker bands in *lane 7* (IMR-32). A map of the probe indicating the transcription initiation site identified by primer extension (*+1*), the labeling site (*), and exons 1 and 2, is shown at the *bottom*.

are extremely low (Fig. 7*A*) and that the top DDX1 protein band in RB412 cell extracts is smaller in size than the top band from the other cell extracts (Fig. 6).

Two DDX1 protein bands were present in most of the lanes in Fig. 6. The same two bands were detected with antiserum to the C terminus of the DDX1 protein, as well as a third band at ~60 kDa (data not shown). There was no variation in the intensity of the 60-kDa band in *DDX1*-amplified and nonamplified cell extracts. The 60-kDa band probably represents another member of the DEAD box protein family, because the C terminus DDX1 protein used to prepare this antiserum contained seven of the eight conserved motifs found in all DEAD box proteins. To obtain an estimate of the size of the two DDX1 bands, we ran cellular extracts from RB522A on a 7% SDS-PAGE gel with the BenchMark protein ladder (Life Technologies, Inc.). The size of the DDX1 protein was determined using the Alpha Imager 2000 documentation and analysis system for molecular weight calculation. Based on this analysis, the estimated molecular mass of the top band is 89.5 kDa, while that of the bottom band is 83.5 kDa. The 84-kDa band may represent the unmodified product encoded by the DDX1 transcript (capable of encoding a protein with a predicted molecular mass of 82.4 kDa), while the top band may represent post-translational modification of DDX1 protein (*e.g.* phosphorylation). Another possibility is that the top band represents intact DDX1

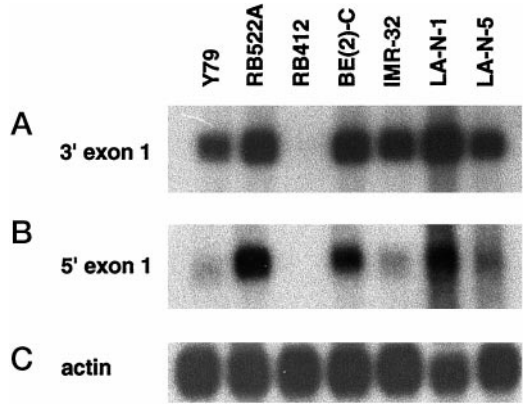

FIG. 5. **Northern blot analysis of the 5′-end of the *DDX1* transcript.** Two μg of poly(A)$^+$ RNA isolated from *DDX1*-amplified Y79, RB522A, BE(2)-C, IMR-32, LA-N-1, and LA-N-5 and nonamplified RB412 were electrophoresed in a 1.5% agarose-formaldehyde gel. The RNA was transferred to a nitrocellulose filter and sequentially hybridized with a 260-bp fragment from *DDX1* cDNA from bp +160 to +420 (3′-end of exon 1 as well as exons 2 and 3) (*A*), a 160-bp fragment from *DDX1* cDNA from bp +1 to +160 (5′-end of exon 1) (*B*), and actin cDNA (*C*). The DNA was labeled with [^{32}P]dCTP by nick translation. The blots were hybridized and washed under high stringency.

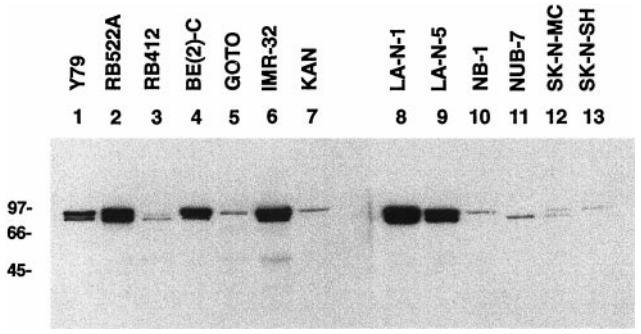

FIG. 6. **DDX1 protein expression in RB and NB cell lines.** Western blots were prepared using total cellular extracts from three RB (Y79, RB522A, and RB412) and 10 NB cell lines (BE(2)-C, GOTO, IMR-32, KAN, LA-N-1, LA-N-5, NB-1, NUB-7, SK-N-MC, and SK-N-SH). The lines that are amplified for the *DDX1* gene are Y79, RB522A, BE(2)-C, IMR-32, LA-N-1, and LA-N-5. Twenty μg of protein were loaded in each lane and electrophoresed in a 10% SDS-PAGE gel. DDX1 was detected using a 1:5000 dilution of the antiserum to the amino terminus of DDX1 protein. Size markers in kilodaltons are indicated on the *side*.

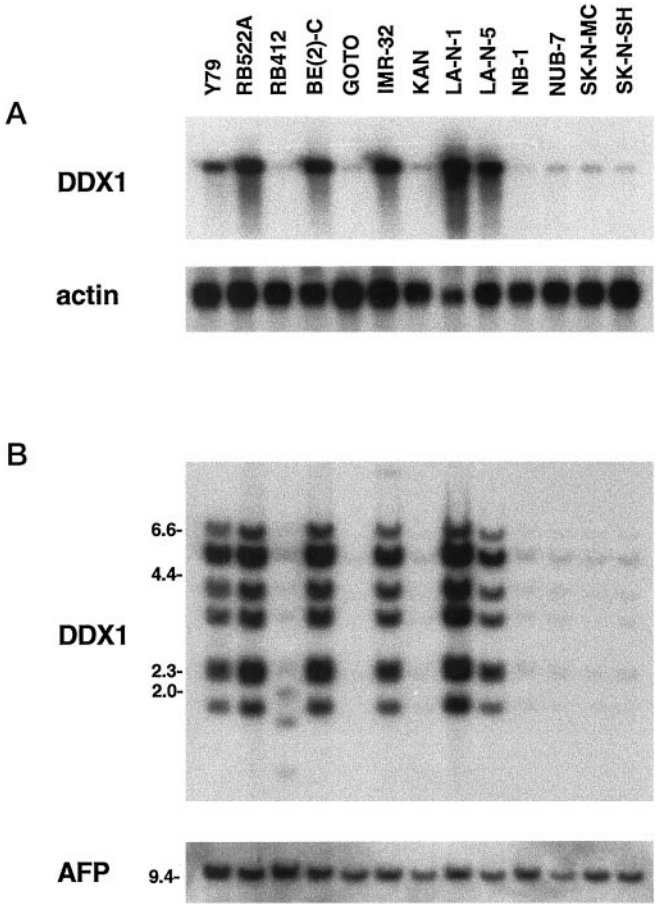

FIG. 7. **Northern and Southern blot analyses of *DDX1* in RB and NB cell lines.** *A*, 2 μg of poly(A)$^+$ RNA were loaded in each lane, electrophoresed in a 1.5% agarose-formaldehyde gel, and transferred to a nitrocellulose filter. The filter was first hybridized to a ^{32}P-labeled 1.6-kb DDX1 cDNA (clone 1042) (21), stripped, and rehybridized to actin DNA. *B*, 10 μg of genomic DNA from each of the indicated cell lines were digested with *Eco*RI, electrophoresed in a 1% agarose gel, and transferred to a nitrocellulose filter. The filter was hybridized to ^{32}P-labeled clone 1042 *DDX1* cDNA, stripped, and reprobed with labeled α-fetoprotein cDNA. Markers (in kilobase pairs) are indicated on the *side*.

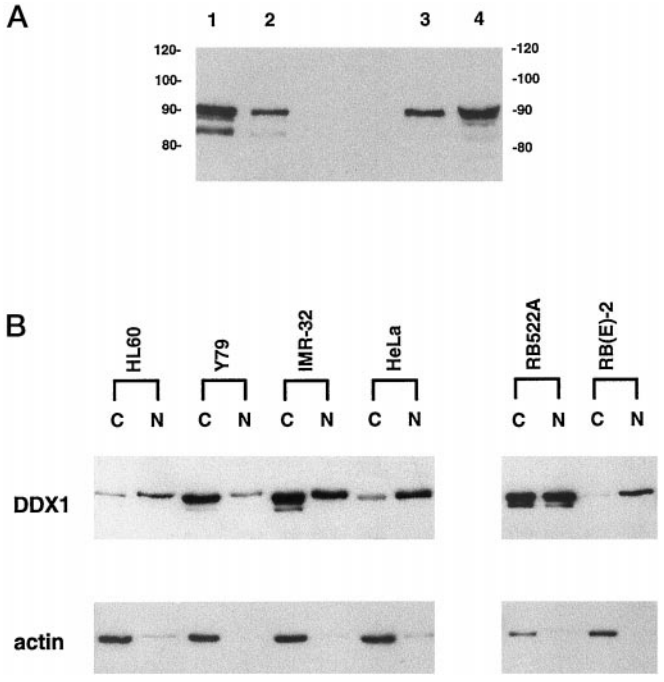

FIG. 8. **Distribution of DDX1 in the nucleus and cytoplasm.** *A*, cytosolic and nuclear extracts were prepared from RB522A and electrophoresed in a 7% SDS-PAGE gel. Cytosolic extracts were loaded in *lanes 1* (20 μg of protein) and *2* (10 μg), while nuclear extracts were loaded in *lanes 3* (10 μg) and *4* (20 μg). DDX1 was visualized using a 1:5000 dilution of the antiserum to the N terminus. The BenchMark protein ladder size markers (kilodaltons) are indicated on the *left*. *B*, cytosolic and nuclear extracts were prepared from HL60, Y79, IMR-32, HeLa, RB522A, and RB(E)-2 and electrophoresed in an 8% SDS-PAGE gel. Twenty μg of proteins were loaded in each *lane* marked *C* (cytosolic) and *N* (nuclear). DDX1 was visualized using a 1:5000 dilution of the antiserum to the N terminus. Actin levels were analyzed using a 1:200 dilution of anti-actin antibody (Santa Cruz Biotechnology).

and the lower band is a specific truncated or degradation product of DDX1. Yet a third possibility is that the two bands represent the products of differentially spliced transcripts or different translation initiation sites. However, the lack of any obvious differences in *DDX1* transcript sizes in the three RB and 10 NB lines analyzed in Fig. 7*A* does not support the latter possibility (*e.g.* compare the *DDX1* transcript size in NUB-7 (which produces the lower DDX1 protein band) and in NB-1 (which produces the higher DDX1 protein band)).

Subcellular Localization of DDX1 Protein—DEAD box proteins have been implicated in a variety of cellular functions including RNA splicing in the nucleus, translation initiation in the cytoplasm, and ribosome assembly in the nucleolus. To obtain an indication of the possible role of DDX1, we studied its subcellular location. Nuclear and cytosolic extracts were prepared from *DDX1*-amplified RB522A and run on a 7% SDS-PAGE gel. Although there was more DDX1 protein in the cytosol than in the nucleus on a per cell basis, the proportion of DDX1 protein relative to total protein was similar in both cellular compartments (Fig. 8*A*). Both the 90- and 84-kDa bands were present in cytosol and nuclear extracts, although the bottom band was more readily apparent in the cytosol. By running the gel for an extended period of time (twice as long as usual), we were able to detect an additional weak band at ~88 kDa in both nuclear and cytosolic extracts.

To determine whether DDX1 consistently localizes to both the cytoplasm and nucleus, we prepared cytosol and nuclear extracts from two additional *DDX1*-amplified lines, Y79 and IMR-32, as well as from nonamplified RB(E)-2, HL60, and HeLa. DDX1 protein was found in both the nucleus and cytoplasm of IMR-32, primarily in the cytoplasm of Y79, and mainly in the nucleus of the three nonamplified lines (Fig. 8*B*). In addition, DDX1 was almost exclusively found in nuclear

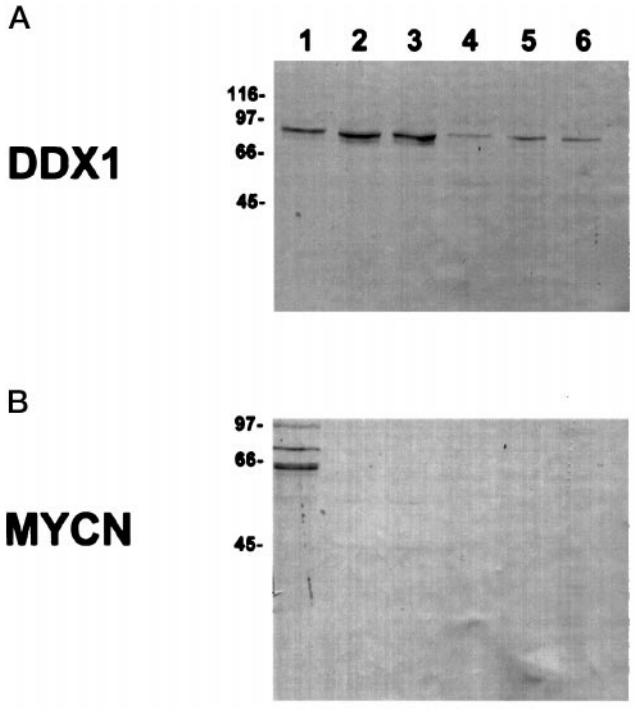

FIG. 9. **Subcellular location of DDX1 protein.** RB522A cells were fractionated into nuclear (*lane 1*), S100 and S4 cytosol (*lanes 2* and *3*), P2 membrane (*lane 4*), P3 membrane (*lane 5*), and P4 membrane (*lane 6*) fractions. Twenty μg of protein were loaded in each lane and run on a 10% SDS-PAGE gel. *A*, DDX1 protein was detected using a 1:5000 dilution of the antiserum to the N terminus of DDX1. *B*, MYCN protein was detected using a commercially available antibody at a 1:200 dilution. Size markers (kilodaltons) are indicated on the *side*.

extracts prepared from normal GM38 fibroblasts (data not shown). We used anti-actin antibody to ensure that our nuclear and cytosolic extracts were not cross-contaminated (Fig. 8*B*).

We next carried out a more detailed analysis of DDX1 subcellular location using two different approaches: (i) fractionation of cellular components into nuclei; S100 or S4 cytosol (containing soluble cytoplasmic components, including 40 S ribosomes); P2 (heavy mitochondria, plasma membrane fragments plus material trapped by these membranes); P3 (mitochondria, lysosomes, peroxisomes, Golgi membranes, some rough endoplasmic reticulum); and P4 (microsomes from smooth and rough endoplasmic reticulum, Golgi and plasma membranes) (43); and (ii) immunogold electron microscopy. The *DDX1*-amplified RB522A cell line was used for both experiments. The fractionation procedures indicate that DDX1 is mainly in the nucleus and in the cytosol (S4 and S100 fractions) of RB522A cells (Fig. 9*A*). As a control, we used anti-human MYCN antibody to determine the location of MYCN (also amplified in RB522A) in our subcellular fractions. As shown in Fig. 9*B*, MYCN was primarily found in the nucleus, as one would expect of a transcription factor.

For the electron microscopy analysis, antiserum to the N terminus of DDX1 was coupled to protein A gold particles, and the distribution of DDX1 was examined in RB522A cells fixed in paraformaldehyde and glutaraldehyde. DDX1 was present in both the cytoplasm and nucleus (data not shown). There was no association with either cell organelles or with nuclear or plasma membranes.

DISCUSSION

There are presently few clues as to the function of DDX1 in normal and cancer cells. Our earlier data indicate that *DDX1* mRNA is present at higher levels in fetal tissues of neural origin (retina and brain) compared with other fetal tissues (21). There may therefore be a requirement for elevated levels of this putative RNA helicase for the efficient production or processing of neural specific transcripts. A role in cancer formation or progression is an intriguing possibility, because overexpression of an RNA unwinding protein could affect the secondary structure of RNAs in such a way as to alter the expression of specific proteins in tumor cells. *DDX1* is co-amplified with *MYCN* in a subset of RB and NB cell lines and tumors (37–39). *MYCN* amplification is common in stage IV NB tumors and is a well documented indicator of poor prognosis. A general trend toward a poorer clinical prognosis is observed when both the *MYCN* and *DDX1* genes are amplified compared with when only *MYCN* is amplified (38, 39), suggesting a possible role for DDX1 in NB tumor formation or progression.

It is generally accepted that co-amplified genes are not overexpressed unless they provide a selective growth advantage to the cell (48, 49). For example, although *ERBA* is closely linked to *ERBB2* in breast cancer and both genes are commonly amplified in these tumors, *ERBA* is not overexpressed (48). Similarly, three genes mapping to 12q13–14 (*CDK4*, *SAS*, and *MDM2*) are overexpressed in a high percentage of malignant gliomas showing amplification of this chromosomal region, while other genes mapping to this region (*GADD153*, *GLI*, and *A2MR*) are rarely overexpressed in gene-amplified malignant gliomas (50, 51). The first three genes are probably the main targets of the amplification process, while the latter three genes are probably incidentally included in the amplicons. The data shown here indicate that DDX1 is overexpressed at both the protein and RNA levels in *DDX1*-amplified RB and NB cell lines and that there is a strong correlation between *DDX1* gene copy number, *DDX1* RNA levels, and DDX1 protein levels in these lines. Our results are therefore consistent with DDX1 overexpression playing a positive role in some aspect of NB and RB tumor formation or progression. Recently, Weiss *et al*. (52) have shown that transgenic mice that overexpress MYCN develop NB tumors several months after birth. They conclude that MYCN overexpression can contribute to the initiation of tumorigenesis but that additional events are required for tumor formation. Amplification of *DDX1* may represent one of many alternative pathways by which a normal precursor "neuroblast" or "retinoblast" cell gains malignant properties.

The function of the majority of tissue-specific or developmentally regulated DEAD box genes remains unknown. However, some members of this protein family have been either directly or indirectly implicated in tumorigenesis. For example, the p68 gene has been found to be mutated in the ultraviolet light-induced murine tumor 8101 (53), while DDX6 (also known as RCK or p54) is encoded by a gene located at the breakpoint of the translocation involving chromosomes 11 and 14 in a cell line derived from a B-cell lymphoma (54, 55). Similarly, the production of a chimeric protein between *DDX10* and the nucleoporin gene *NUP98* has been proposed to be involved in the pathogenesis of a subset of myeloid malignancies with inv(11) (p15q22) (56). Interestingly, Grandori *et al*. (57) have shown that MYCC interacts with a DEAD box gene called *MrDb*, suggesting that the transcription of some DEAD box genes could be regulated through interaction with members of the MYC family. Future work will involve determining whether DDX1 represents another member of the DEAD box family with a role in the tumorigenic process.

DEAD box proteins have been implicated in translation initiation, RNA splicing, RNA degradation, and RNA stability (3, 18, 19). We carried out subcellular localization studies in an attempt to obtain a general indication of the function of DDX1. We found DDX1 protein in both the cytoplasm and nucleus of *DDX1*-amplified NB and RB lines. In contrast, DDX1 was

mainly located in the nucleus of nonamplified cell lines and normal fibroblast cultures. DDX1 was not associated with cellular organelles or with membranes based on immunoelectron microscopy. We therefore propose that the primary role of DDX1 is in the nucleus. The presence of DDX1 in the cytoplasm of *DDX1*-amplified cells may indicate that the amount of DDX1 protein that is allowed in the nucleus is tightly regulated. Alternatively, DDX1 may play a dual role in the nucleus and cytoplasm of *DDX1*-amplified cells.

An important component of our analysis was to identify the translation and transcription initiation sites of *DDX1*. We used a combination of techniques to identify the transcription start site: screening of RB and fetal brain libraries, RACE, primer extension, genomic DNA sequencing, S1 nuclease mapping, and Northern blot analysis using probes to the predicted 5′-end of the transcript. The transcription start site identified using these techniques is located ~300 nt upstream of the predicted translation initiation codon and was readily detected in three *DDX1*-amplified lines and barely detectable in a fourth amplified line. The 5′-untranslated region as well as the first in frame methionine are encoded within the first exon of *DDX1*. An in frame stop codon is located 123 nt upstream of the predicted initiation codon. We were unable to identify the transcription initiation site of *DDX1* in two of the six amplified lines tested as well as in nonamplified lines. Although it remains possible that there are different transcription start sites in different cell lines, detection of lower levels (rather than the absence) of the 5′-most 160 nt of the *DDX1* transcript in IMR-32, Y79, and LA-N-5 compared with RB522A, BE(2)-C, and LA-N-1 supports a quantitative rather than a qualitative difference in the 5′-end of this transcript in these cells. Our results suggest that the 5′-end of *DDX1* mRNA is rarely intact, even in mRNA preparations that otherwise appear to be of high quality based on analysis of control transcripts. The 5′-end of *DDX1* mRNA may therefore be especially susceptible to degradation, perhaps because of its sequence and/or secondary structure.

In conclusion, we have mapped the 5′-end of the 2.7-kb *DDX1* transcript and have identified the predicted translation initiation site of DDX1 protein. We have found that *DDX1*-amplified RB and NB tumor lines overexpress DDX1 protein and that there is a good correlation between gene copy number and both transcript and protein levels in these cells. We have shown that DDX1 protein is primarily located in the nucleus of cells that are not *DDX1*-amplified. In contrast, DDX1 is present in both the nucleus and cytoplasm of *DDX1*-amplified NB and RB lines. A cytoplasmic location in *DDX1*-amplified lines may indicate that the amount of nuclear DDX1 is tightly regulated or that DDX1 plays a dual role in the cytoplasm and nucleus of these cells.

Acknowledgments—We thank Walter Dixon, Brenda Gallie, Ajay Pandita, Jeremy Squire, and Herman Yeger for the neuroblastoma and retinoblastoma cell lines. We thank Halyna Marusyk for carrying out the electron microscopy analyses. We are grateful to Randy Andison for expert help in the preparation of the manuscript and to Stacey Hume for helpful discussions.

REFERENCES

1. Linder, P., Lasko, P. F., Ashburner, M., Leroy, P., Nielsen, P. J., Nishi, K., Schnier, J., and Slonimski, P. P. (1989) *Nature* **337,** 121–122
2. Wassarman, D. A., and Steitz, J. A. (1991) *Nature* **349,** 463–464
3. Schmid, S. R., and Linder, P. (1992) *Mol. Microbiol.* **6,** 283–292
4. Rozen, F., Edery, I., Meerovitch, K., Dever, T. E., Merrick, W. C., and Sonenberg, N. (1990) *Mol. Cell. Biol.* **10,** 1134–1144
5. Hirling, H., Scheffner, M., Restle, T., and Stahl, H. (1989) *Nature* **339,** 562–564
6. Liang, L., Diehl-Jones, W., and Lasko, P. (1994) *Development* **120,** 1201–1211
7. Gururajan R., Mathews, L., Longo, F., and Weeks, D. L. (1994) *Proc. Natl. Acad. Sci.* U. S. A. **91,** 2056–2060
8. Dalbadie-McFarland, G., and Abelson, J. (1990) *Proc. Natl. Acad. Sci. U. S. A.* **87,** 4236–4240
9. Jamieson, D. J., Rahe, B., Pringle, J., and Beggs, J. D. (1991) *Nature* **349,** 715–717
10. Strauss, E. J., and Guthrie, C. (1994) *Nucleic Acids Res.* **22,** 3187–3193
11. Nishi, K., Morel-Deville, F., Hershey, J. W. B., Leighton, T., and Schnier, J. (1988) *Nature* **336,** 496–498
12. Leroy, P., Alzari, P., Sassoon, D. Wolgemuth, D., and Fellous, M. (1989) *Cell* **57,** 549–559
13. Hay, B., Jan, L. Y., and Jan, Y. N. (1988) *Cell* **55,** 577–587
14. De Valoir, T., Tucker, M., Belikoff, E. J., Camp, L. A. Bolduc, C., and Beckingham, K. (1991) *Proc. Natl. Acad. Sci. U. S. A.* **88,** 2113–2117
15. Ford, M. J., Anton, I. A., and Lane, D. P. (1988) *Nature* **332,** 736–738
16. Iggo, R. D., and Lane, D. P. (1989) *EMBO J.* **8,** 1827–1831
17. Buelt, M. K., Glidden, B. J., and Storm, D. R. (1994) *J. Biol. Chem.* **269,** 29367–29370
18. Iost, I., and Dreyfus, M. (1994) *Nature* **372,** 193–196
19. Py, B., Higgins, C. F., Krisch, H. M., and Carpousis, A. J. (1996) *Nature* **381,** 169–172
20. Missel, A., Souza, A. E., Nörskau, G., and Göringer, H. U. (1997) *Mol. Cell. Biol.* **17**, 4895–4903
21. Godbout, R., and Squire, J. (1993) *Proc. Natl. Acad. Sci. U. S. A.* **90,** 7578–7582
22. Kiledjian, M., and Dreyfuss, G. (1992) *EMBO J.* **11,** 2655–2664
23. Godbout, R., Hale, M., and Bisgrove, D. (1994) *Gene* (*Amst.*) **138,** 243–245
24. Blackwood, E. M., and Eisenman, R. N. (1991) *Science* **251,** 1211–1217
25. Amati, B., Dalton, S., Brooks, M. W., Littlewood, T. D., Evan, G. I., and Land, H. (1992) *Nature* **359,** 423–426
26. Brodeur, G. M., Seeger, R. C., Schwab, M., Varmus, H. E., and Bishop, J. M. (1984) Science **224,** 1121–1124
27. Seeger, R. C., Brodeur, G. M., Sather, H., Dalton, A., Siegel, S. E., Wong, K. Y., and Hammond, D. (1985) *N. Engl. J. Med.* **313,** 1111–1116
28. Cohn, S. L., Salwen, H., Quasney, M. W., Ikegaki, N., Cowan, J. M., Herst, C. V., Sharon, B., Kennett, R. H., and Rosen, S. T. (1991) *Prog. Clin. Biol. Res.* **366,** 21–27
29. Cowell, J. K. (1982) *Annu. Rev. Genet.* **16,** 21–59
30. Zehnbauer, B. A., Small, D., Brodeur, G. M. Seeger, R., and Vogelstein, B. (1988) *Mol. Cell. Biol.* **8,** 522–530
31. Akiyama, K., and Nishi, Y. (1991) *Nucleic Acids Res.* **19,** 6887–6894
32. Schneider, S. S., Hiemstra, J. L., Zehnbauer, B. A., Taillon-Miller, P., Le Paslier, D., Vogelstein, B., and Brodeur, G. M. (1992) *Mol. Cell. Biol.* **12,** 5563–5570
33. Amler, L. C., Schürmann, J., and Schwab, M. (1996) *Genes Chromosomes Cancer* **15,** 134–137
34. Kuroda, H., White, P. S., Sulman, E. P., Manohar, C., Reiter, J. L., Cohn, S. L., and Brodeur, G. M. (1996) *Oncogene* **13,** 1561–1565
35. Noguchi, Y., Akiyama, K., Yokoyama, M., Kanda, N., Matsunaga, T., and Nishi, Y. (1996) *Genes Chromosomes Cancer* **15,** 129–133
36. Pandita, A., Godbout, R., Zielenska, M., Thorner, P., Bayani, J., and Squire, J. A. (1997) *Genes Chromosomes Cancer* **20,** 243–252
37. Manohar, C. F., Salwen, H. R., Brodeur, G. M., and Cohn, S. L. (1995) *Genes Chromosomes Cancer* **14,** 196–203
38. Squire, J. A., Thorner, P. S., Weitzman, S., Maggi, J. D., Dirks, P., Doyle, J., Hale, M., and Godbout, R. (1995) *Oncogene* **10,** 1417–1422
39. George, R. E., Kenyon, R. M., McGuckin, A. G., Malcolm, A. J., Pearson, A. D. J., and Lunec, J. (1996) *Oncogene* **12,** 1583–1587
40. Reiter, J. L., and Brodeur, G. M. (1996) *Genomics* **32,** 97–103
41. Favaloro, J., Treisman, R., and Kamen, R. (1980) *Methods Enzymol.* **65,** 718–745
42. Dignam, J. D. (1990) *Methods Enzymol.* **182,** 194–203
43. Graham, J. (1984) in *Centrifugation: A Practical Approach* (Rickwood, D. ed.) 2nd Ed., pp. 161–182, IRL Press, Oxford
44. Godbout, R., Marusyk, H., Bisgrove, D., Dabbagh, L., and Poppema, S. (1995) *Exp. Eye Res.* **60,** 645–657
45. Miller, K. G., and Sollner-Webb, B. (1981) *Cell* **27,** 165–174
46. Kozak, M. (1988) *Nucleic Acids Res.* **15,** 8125–8132
47. Rafti, F., Scarvelis, D., and Lasko, P. F. (1996) *Gene* (*Amst.*) **171,** 225–229
48. Van de Vijver, M., van de Bersselaar, R., Devilee, P., Cornelisse, C., Peterse, J., and Nusse, R. (1987) *Mol. Cell. Biol.* **7,** 2019–2023
49. Gaudray, P., Szepetowski, P., Escot, C., Birnbaum, D., and Theillet, C. (1992) *Mutat. Res.* **276,** 317–328
50. Forus, A., Florence, V. A., Maelandsmo, G. M., Meltzer, P. S., Fodstad, O., and Myklebost, O. (1993) *Cell Growth Differ.* **4,** 1065–1070
51. Reifenberger, G., Reifenberger, J., Ichimura, K., Meltzer, P. S., and Collins, V. P. (1994) *Cancer Res.* **54,** 4299–4303
52. Weiss, W. A., Aldape, K., Mohapatra, G., Feuerstein, B. G., and Bishop, J. M. (1997) *EMBO J.* **16,** 2985–2995
53. Dubey, B. P., Hendrickson, R. C., Meredith, S. C., Siegel, C. T., Shabanowitz, J., Skipper, J. C. A., Engelhard, V. H., Hunt, D. F., and Schreiber, H. (1997) *J. Exp. Med.* **185,** 695–705
54. Akao, Y., Seto, M., Yamamoto, K., Iida, S., Nakazawa, S., Inazawa, J., Abe, T., Takahashi, T., and Ueda, R. (1992) *Cancer Res.* **52,** 6083–6087
55. Lu, D., and Yunis, J. J. (1992) *Nucleic Acids Res.* **20,** 1967–1972
56. Arai, Y., Hosoda, F., Kobayashi, H., Arai, K., Hayashi, Y., Kamada, N., Kaneko, Y., and Ohki, M. (1997) *Blood* **89,** 3936–3944
57. Grandori, C., Mac, J., Siëbelt, F., Ayer, D. E., and Eisenman, R. N. (1996) *EMBO J.* **15**, 4344–4357